Progress In Electromagnetics Research C, Vol. 38, 115–128, 2013

DIELECTRIC RESONATOR ANTENNA REFLECTARRAYS MOUNTED ON OR EMBEDDED IN CONFORMAL SURFACES

Saber H. Zainud-Deen[1], Noha A. El-Shalaby[2], Hend A. Malhat[1, *], Shaymaa M. Gaber[3], and Kamal H. Awadalla[1]

[1]Faculty of Electronic Eng., Menoufia University, Egypt

[2]Kafer El-Sheikh University, Egypt

[3]Egyptian Russian University, Egypt

Abstract—In this paper, reflectarrays mounted on or embedded in cylindrical and spherical surfaces are designed, analyzed, and simulated at 11.5 GHz for satellite applications. A unit cell consists of a square dielectric resonator antenna (DRA) mounted on or embedded in metallic conformal ground plane is investigated. The radiation characteristics of the designed reflectarrays are investigated and compared with that of planar reflectarray. A 13×13 planar reflectarray antenna on the x-y plane was designed. By varying the length of the DRA element between 2 mm and 6.2 mm a full range from 0° to 360° phase shift can be obtained. The size of each element is equivalent to a compensation phase shift. A maximum directivity of 24.3 dB was achieved while the side lobes were below −12.94 dB in E-plane and −15.79 dB in the H-plane for planar reflectarray. A Full-wave analysis using the finite integration technique (FIT) is applied. The results are validated by comparing with that calculated by transmission line method (TLM).

1. INTRODUCTION

A reflectarray antenna combines the advantages of both printed arrays and reflector antennas, and has low-profile, low mass, and low cost features [1–4]. The reflectarray consists of an array of unit-cells illuminated by a primary feed. Each unit-cell designed

Received 24 February 2013, Accepted 20 March 2013, Scheduled 21 March 2013

* Corresponding author: Hend Abd El-Azem Malhat (er_honida1@yahoo.com).

in such a way as to correct the phase of the incident wave as is done in the traditional parabolic reflector. The reflectarray has received considerable attention over the years and is quickly finding many applications [5–7]. There are several methods for reflectarray elements design to achieve a planar phase front. For example, one is to use identical microstrip patches with different-length phase-delay lines attached so that they can compensate for the phase delays over the different paths from the illuminating feed. The other is to use variable-size patches, dipoles, or rings so that elements can have different scattering impedances and, thus, different phases to compensate for the different feed-path delays [8]. To combat the shortcoming of narrow bandwidth of the reflectarray, dual-band multilayer reflectarrays using variable patch size, annular rings, and crossed dipoles are also being developed. Various reflectarray approaches have been described in the literature [9]. In the last decade, most of the work on reflectarray structures has concentrated on planar reflectarray. However, reflectarray on cylindrical and spherical surfaces are a basic one in many important practical problems. The use of reflectarray on cylindrical surfaces may be of particular importance for satellites. Low profile printed antennas flush mounted on curved surfaces such as cylinders and spheres represents an important class of conformal arrays that have been used in radar and communication systems [10]. Cylindrical array antennas are mainly utilized when full azimuth scanning is required, however in many practical applications where a curved platform is available, such as missiles, ships and aircrafts, full azimuth scanning is not required [11, 12]. For these applications, sector arrays, where the elements occupy a sector of subtended angle are appropriate [1]. The aim of this study is to investigate the feasibility of designing sector reflectarrays on conformal cylindrical and spherical surfaces. Dielectric resonators antenna (DRA) were used as the cell antenna element in designing the reflectarrays to improve the bandwidth of the reflectarray due to their low loss, high radiation efficiency and low mutual coupling between the elements [13–15]. The performance of these reflectarrays are compared with planar designs.

In this paper, cylindrical and spherical reflectarrays are designed and analyzed. The performance of the antenna is verified through modelling and simulation using the finite integration technique (FIT) [16] and the results are compared with that calculated using the transmission line model technique (TLM) [17] and the finite element method (FEM) [18].

2. NUMERICAL RESULTS

2.1. Planar Reflectarray

Consider that a square dielectric resonator antenna (DRA) is placed on a square perfect ground plane of length $L_c = 15\,\text{mm}$ as depicted in Fig. 1(a). The structure is used as a unit-cell for the planar reflectarray. The dimensions of the DRA are length L that varies according to its position in the array, and height $H_d = 3\,\text{mm}$, with relative dielectric constant of the material used for the DRA, $\varepsilon_r = 10.2$. The structure was placed in a $15\,\text{mm} \times 15\,\text{mm}$ waveguide with boundary conditions for the side walls to simulate an infinite periodic structure. The cell is inserted in the middle of the waveguide simulator as shown in Fig. 1(b). The perfect electric and magnetic wall boundary conditions are applied to the sides of the surrounding waveguide, and result in image planes on all sides of the unit cell [9]. The produced electric field from the element is chosen normal to the perfect electric conductor wall where $E_{\text{tang}} = 0$, while the produced magnetic field from the element is chosen normal to the perfect magnetic conductor wall where $H_{\text{tang}} = 0$. In this manner, the cell element is repeated to infinity in the simulator. There are several limitations to the infinite array approach. First, all elements of the array are identical; this is clearly not the case in a real reflectarray in which the cell element must vary according to the phase compensation required. Secondly, the reflectarray itself is not infinite in extent. Consequently, edge effects such as diffraction are not accounted for in the simulation. A normal incident plane wave incident on a periodic infinite array of the DRA elements was assumed to determine the reflection coefficient of one element. By varying the length of the DRA element between 2 mm and 6.2 mm a full range from 0° to 360° phase shift can be obtained as shown in Fig. 1(c). The results are determined using the FEM and are compared with that calculated using the TLM. The results obtained with the two techniques agree well. Based on the required phase distribution, the curve in Fig. 1(b) can be used to determine the required length of the individual DRA elements composing the reflectarray. Using this unit-cell element, a 13×13 planar reflectarray antenna on the x-y plane was designed. The Phase-shift φ_R required at each unit cell in the reflectarray in x-y plane is obtained as in Eq. (1):

$$\begin{aligned} &\varphi_R(x_{ce}, y_{ce}, z_{ce}) \\ &= k_o[d_i - x_{ce}\sin(\theta_o)\cos(\phi_o) - y_{ce}\sin(\theta_o)\sin(\phi_o) - z_{ce}\cos(\phi_o)] \end{aligned} \quad (1)$$

$$d_i = \sqrt{(x_{ce} - x_f)^2 + (y_{ce} - y_f)^2 + (z_{ce} - z_f)^2} \quad (2)$$

where $k_0 = 2\pi/\lambda_0$ is the propagation constant in free space; (x_{ce}, y_{ce}, z_{ce}) are the coordinates of reflectarray unit cell; (x_f, y_f, z_f) are the coordinates of feeding element; (θ_o, ϕ_o) is the desired direction of the reflected main beam as shown in Fig. 2. The size of each element is equivalent to a compensation phase shift. When the DRA size approaches the minimum value given in Fig. 1(c) (2 mm), an additional phase shift of 2π is added in order to produce realizable DRA sizes, which explain the sudden jump in the variation of the DRA element size as shown in Fig. 1(a).

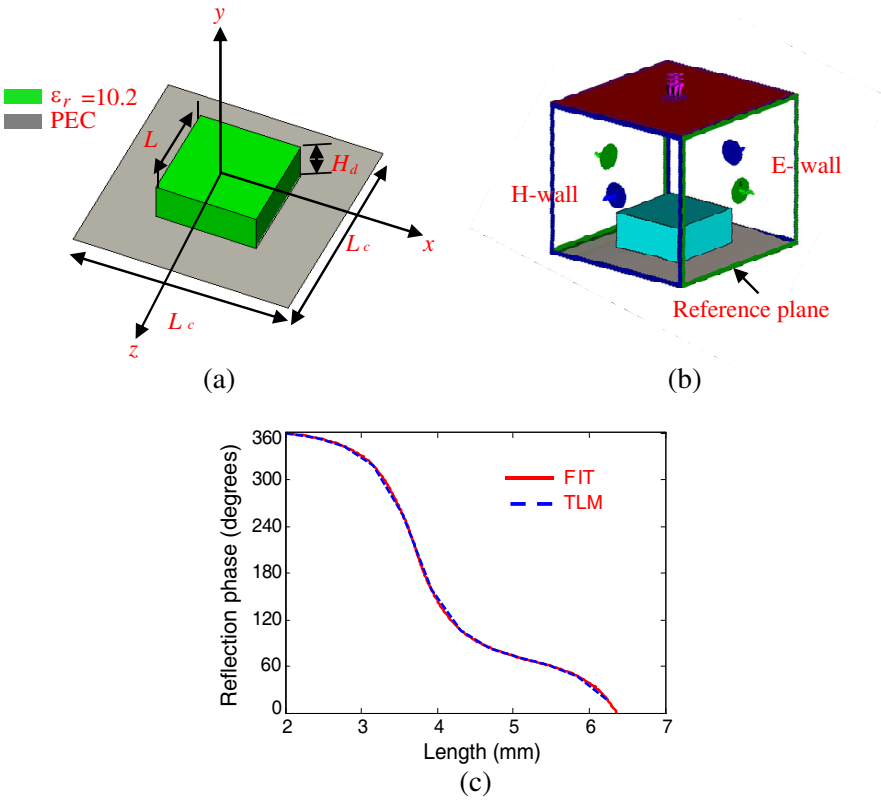

Figure 1. The geometry of a Planar unit cell element and its reflection coefficient phase variation versus DRA length. (a) The structure of unit cell. (b) The waveguide simulator. (c) Reflection phase versus length, L.

The antenna size was 19.5 cm × 19.5 cm. A linearly polarized pyramidal horn with an aperture size of 60 mm × 30 mm and 45 mm

long is used as the feed. The antenna was centre fed, with the main beam at 0°. The working frequency of the reflectarray is going to be 11.5 GHz and the focal-length-to-diameter ratio, F/D was set to one. Theoretical gain patterns in yz plane (E-plane) and xz plane (H-plane) using the FEM and TLM techniques are shown in Fig. 3. Good concordance between FIT and TLM results is obtained. A maximum directivity of 24.3 dB was achieved while the side lobes were below −12.94 dB in E-plane and −15.79 dB in the H-plane. The gain as a function of frequency is shown in Fig. 4. A 8.7 % bandwidth (1 GHz) is achieved with 1 dB gain variations. This is mainly due to the wideband of the DRA.

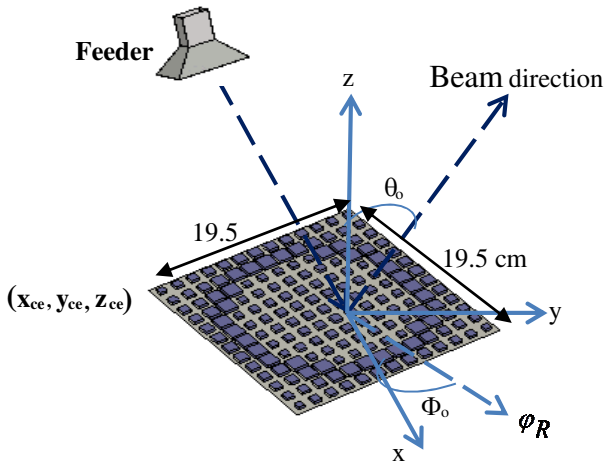

Figure 2. The geometry of DRA reflectarray.

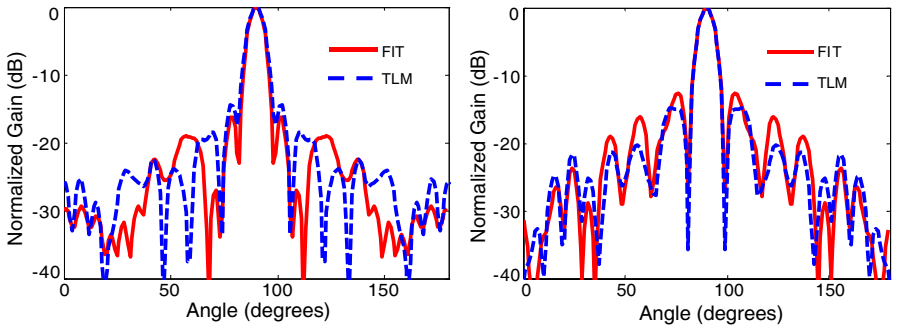

Figure 3. 13 × 13 planar reflectarray normalized gain patterns at 11.5 GHz. (a) H-plane (yz-plane). (b) E-plane (xy-plane).

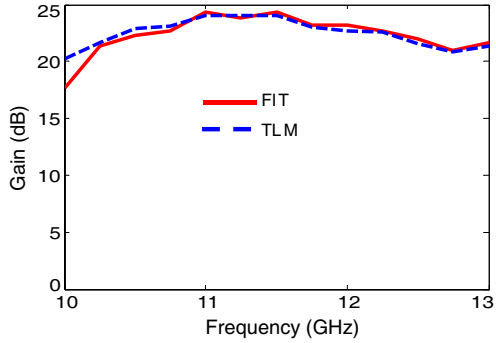

Figure 4. Gain versus frequency for 13×13 planar reflectarray.

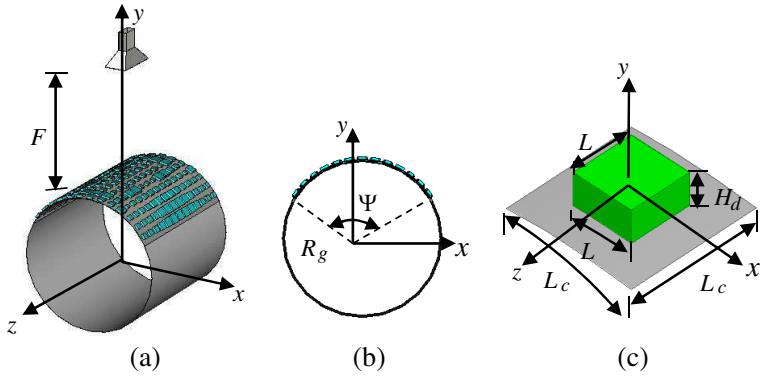

Figure 5. Reflectarray mounted on cylindrical surface. (a) 3-D view. (b) Side view. (b) The structure of unit cell.

2.2. Cylindrical Reflectarray

Some applications such as satellites, radars and communication systems need low profile printed antennas on curved surfaces such as cylinders and spheres. Therefore, we designed new structure of the reflectarray on curved structure to be more conformal and suitable for those applications. Fig. 5 shows a 13×13 reflectarray mounted on the cylindrical surface and its individual cell. The radius of the cylinder, $R_g = 124.1$ mm and the subtended angle at the centre, $\psi = 90°$. The arc length of the reflectarray is the same as in planar reflectarray case. The normalized gain patterns for cylindrical reflectarray at $f = 11.5$ GHz is shown in Fig. 6.

The gain as a function of frequency is shown in Fig. 7. A maximum directivity of 21.8 dB was achieved while the side lobes were

below −13 dB in E plane and −14.5 dB in the H-plane. A 8.7% bandwidth is achieved with 1 dB gain variations. Table 1 illustrates a comparison between the radiation characteristics of the planar reflectarray compared with that calculated for reflectarray mounted on the cylindrical structure for different values of subtended angle at the centre ψ. When the curvature is increased (ψ increased and radius decreased) the effective area that is in front of the horn antenna is decreased so the gain is decreased and the gain bandwidth is changed. Cylindrical reflectarray can use instead of planar with little variation of its characteristics as listed in Table 1.

Moderate the previous design (mounted on) to become more protected and more directives by embedding the DRAs elements in

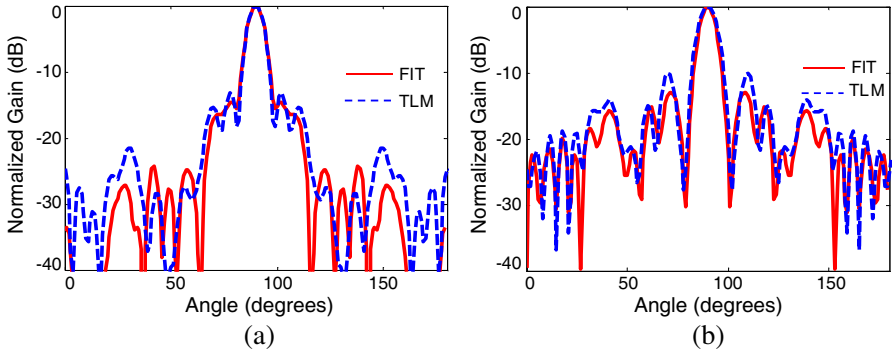

Figure 6. Normalized gain patterns plot for a 13 × 13 reflectarray mounted on cylindrical surface with $R_g = 124.1$ and $\Psi = 90°$ at 11.5 GHz. (a) yz-plane. (b) xy-plane.

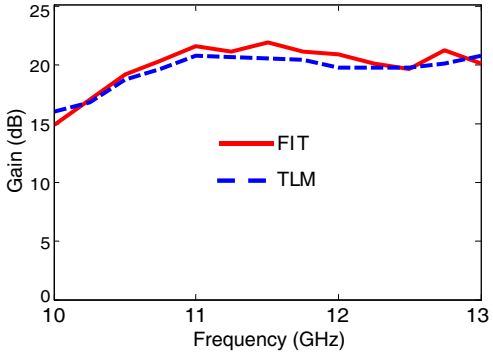

Figure 7. Gain versus frequency for 13 × 13 reflectarray mounted on cylindrical surface with $R_g = 124.1$ and $\Psi = 90°$.

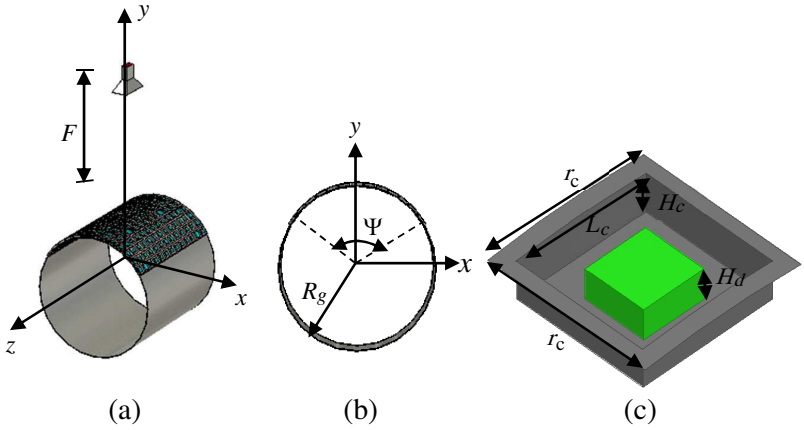

Figure 8. Reflectarray embedded in cylindrical surface. (a) 3-D view. (b) Side view. (c) The structure of unit cell.

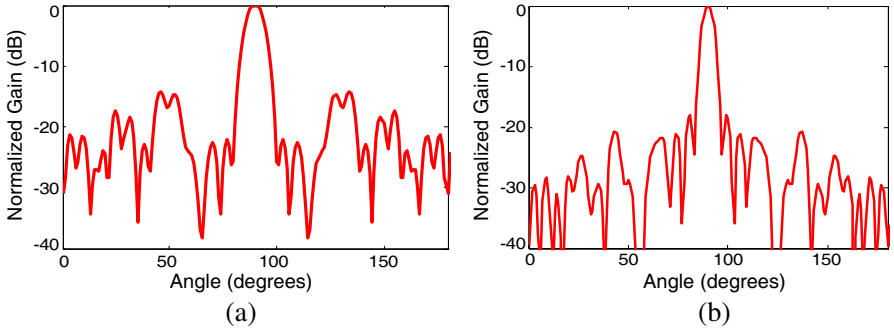

Figure 9. The normalized gain patterns 13×13 reflectarray embedded in cylindrical surface at 11.5 GHz for $\Psi = 90°$. (a) H-plane (yz-plane). (b) E-plane (xy-plane).

cavities coated with different materials as foam in this case, which act as a reflector. Fig. 8 shows a 13×13 reflectarray embedded in the cylindrical surface and its individual cell where the square dielectric resonator antenna embedded in a square perfect ground plane of length $L_c = 15$ mm, $r_c = 18.75$ mm and $H_c = 4$ mm is shown in Fig. 8(c). The radius of the cylinder, $R_g = 149.5$ mm and the subtended angle at the center, $\psi = 90°$. DRA reflectarray embedded in the cylindrical surface at 11.5 GHz according to the phase compensation. The normalized gain patterns for an embedded cylindrical reflectarray at $f = 11.5$ GHz is shown in Fig. 9. Fig. 10 shows the normalized gain as a function of frequency.

Table 1. DRA reflectarray mounted on cylindrical surface.

Ψ	Gain variation (dB)	SLL (yz-plane)	SLL (xy-plane)
Linear	20–22	−12.94	−15.79
$\Psi = 20^o$, $R_g = 558.6\,\text{mm}$	18–21	−12.7	−15.31
$\Psi = 40°$, $R_g = 279.2\,\text{mm}$	17–22	−12.43	−14.02
$\Psi = 60°$, $R_g = 186.3\,\text{mm}$	16–20	−16.52	−14.02
$\Psi = 90°$, $R_g = 124.1\,\text{mm}$	15–20	−13.02	−14.58
$\Psi = 120°$, $R_g = 93.1\,\text{mm}$	14–17	−12.36	−14.02

A maximum directivity of 22.8 dB was achieved while the side lobes were below −18 dB in E-plane and −13 dB in the H-plane. A 7.1% bandwidth is achieved with 1 dB gain variations. Table 2 illustrates a comparison between the radiation characteristics of the planar reflectarray compared with that calculated for reflectarray embedded in the cylindrical structure. The embedded case has increased the gain about 1 dB but decreased the bandwidth due to the effect of the cavity but more complex in fabrication.

Table 2. DRA reflectarray embedded in cylindrical surface.

Ψ	Gain Variation (dB)	SLL (yz-plane)	SLL (xy-plane)
Linear 0°	18–16	−17.3	−11.7
$\Psi = 20°$ $R_g = 698.3\,\text{mm}$	17–16	−15.4	−11.8
$\Psi = 40°$ $R_g = 349.2\,\text{mm}$	16–15	−20.1	−15.2
$\Psi = 60°$ $R_g = 232.8\,\text{mm}$	15–14	−16.1	−15
$\Psi = 90°$ $R_g = 149.5\,\text{mm}$	13–10	−18	−13.3
$\Psi = 120°$ $R_g = 112.1\,\text{mm}$	12.5–5	−14.1	−12.4

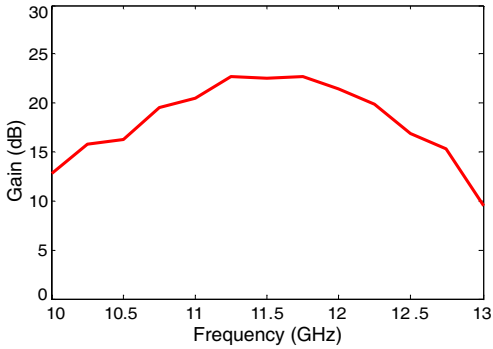

Figure 10. Gain versus frequency for 13×13 reflectarray emdedded in cylindrical surface with $R_g = 124.1$ and $\Psi = 90°$.

2.3. Spherical Reflectarray

In some applications, sometimes low profile antennas are needed to be fixed on spherical objects. A 13×13 reflectarray mounted on spherical surface and its individual unit-cell element is shown in Fig. 11. The radius of the sphere, $R_s = 279.2\,\text{mm}$ and $\psi = 40°$. The normalized gain patterns for a spherical reflectarray at $f = 11.5\,\text{GHz}$ is shown in Fig. 12. The gain versus frequency is shown in Fig. 13. A maximum directivity of 23.01 dB was achieved while the side lobes were below $-12\,\text{dB}$ in E-plane and $-12\,\text{dB}$ in the H-plane. A 8.7% bandwidth is achieved with 1 dB gain variations. Table 3 illustrates a comparison between the radiation characteristics of the spherical reflectarray with different ψ.

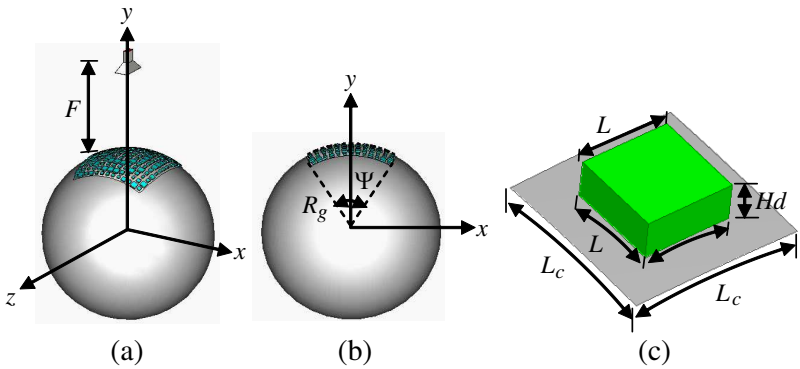

Figure 11. Reflectarray embedded in spherical surface. (a) 3-D view. (b) Side view. (c) The unit cell.

Table 3. DRA reflectarray mounted on spherical surface.

Ψ	Gain Variation (dB)	SLL (yz plane)	SLL (yz plane)
$\Psi = 20^\circ$ $R_g = 558.6\,\text{mm}$	15–22	−11.35	−15.92
$\Psi = 40^\circ$ $R_g = 279.2\,\text{mm}$	14–20	−12.27	−12.27
$\Psi = 60^\circ$ $R_g = 186.306\,\text{mm}$	15–20	−22.85	−19.13

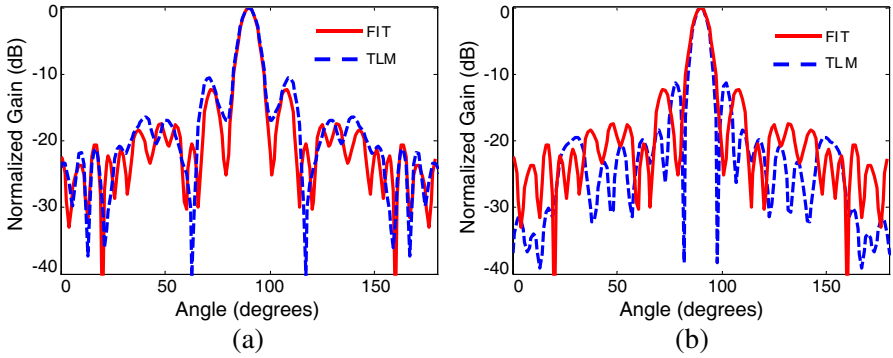

Figure 12. The normalized gain patterns 13×13 reflectarray mounted on spherical surface at 11.5 GHz for $\Psi = 90^\circ$. (a) H-plane (yz-plane). (b) E-plane (xy-plane).

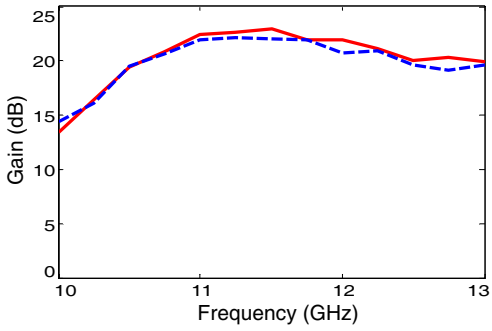

Figure 13. Gain versus frequency for 13×13 reflectarray mounted on spherical surface at $\Psi = 40^\circ$.

Note that the curvature effect on radiation is more in spherical surfaces (the curvature is in all directions) than in cylindrical surfaces, and the effective area exposed to the horn antenna is smaller. Therefore, the directivity and the gain bandwidth are decreased as listed in Table 1 and Table 2. Fig. 14 shows a 13×13 reflectarray embedded in the spherical surface and its individual cell is depicted in Fig. 14(c). The radius of the sphere, $R_s = 349.2\,\text{mm}$ and the $\psi = 40°$. The normalized gain patterns for an embedded spherical reflectarray at $f = 11.5\,\text{GHz}$ is shown in Fig. 15. A maximum directivity of 24.7 dB was achieved while the side lobes were below $-18.7\,\text{dB}$ in E-plane and $-17.3\,\text{dB}$ in the H-plane. A 4.4% bandwidth (0.51 GHz) is achieved with 1 dB gain variations. The embedded case has increased the gain about 1.5 dB but decreased the bandwidth due to the effect of the cavity but the structure is more complex in fabrication.

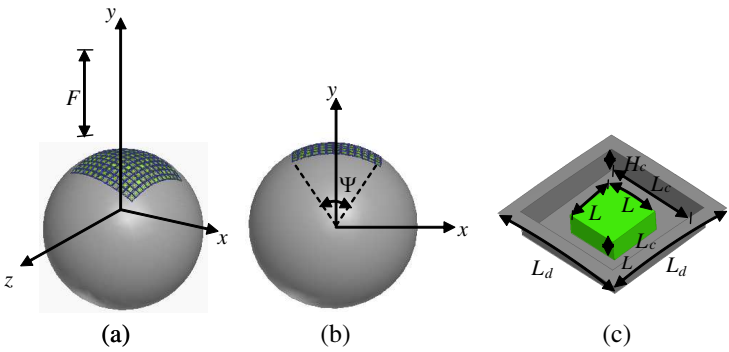

Figure 14. Reflectarray embedded in spherical surface. (a) 3-D view. (b) Side view. (c) The structure of unit cell.

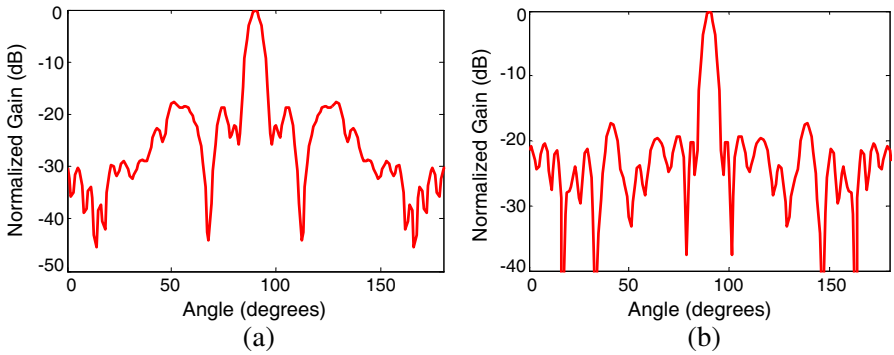

Figure 15. The normalized gain patterns 13×13 reflectarray embedded in spherical surface at 11.5 GHz for $\Psi = 90°$. (a) H-plane (yz-plane). (b) E-plane (xy-plane).

3. CONCLUSIONS

This paper has demonstrated the design of reflectarray mounted on or embedded in cylindrical or spherical reflectarray using DRA elements. The use of reflectarray on cylindrical surfaces may be of particular importance for satellites. Design of embedded structures is introduced to protect the array. DRA antenna elements are chosen in the present design. In order to increase the operational bandwidth of the reflectarray. It is demonstrated that a reflectarray antenna mounted on or embedded in a cylindrical or spherical surfaces can achieve a similar radiation pattern with slight reduction in gain relative to planar surfaces. The embedded structures for all cases gives higher directivity and are more practical than the salient DRAs. When the curvature is increased (ψ increased and radius decreased) the effective area that is in front of the horn antenna is decreased so the gain is decreased and the gain bandwidth is changed. The curvature effect on radiation is more in spherical surfaces (the curvature is in all directions) than in cylindrical surfaces, and the effective area exposed to the horn antenna is smaller. Therefore, the directivity and the gain bandwidth are decreased

REFERENCES

1. Josefsson, L. and P. Persson, *Conformal Array Antenna Theory and Design*, IEE Press Series on Electromagnetic Wave Theory, Wiley-Interscience, 2006.
2. Huang, J. and J. A. Encinar, *Reflectarray Antennas*, John Wiley and Sons, Inc., Hoboken, NJ, USA, 2007.
3. Zainud-Deen, S. H., E. Abd, A. A. Mitkees, and A. A. Kishk, "Design of dielectric resonator reflectarray using full-wave analysis," *National Radio Science Conference*, 1–9, Egypt, 2009.
4. Cadoret, D., L. Marnat, R. Loison, R. Gillard, H. Legay, and B. Salome, "A dual linear polarized printed reflectarray using slot loaded patch elements," *The 2nd European Conference Antenna and Propagation*, 1–5, 2007.
5. Hansen, R. C., *Phased Array Antennas*, John Wiley & Sons, 1998.
6. Abbosh, A. M., "Design of dual-band microstrip reflectarray using single layer multiresonance double cross elements," *Progress In Electromagnetics Research Letters*, Vol. 13, 67–74, 2010.
7. Ren, L.-S., Y.-C. Jiao, F. Li, J.-J. Zhao, and G. Zhao, "A novel double-petal loop element for broadband reflectarray," *Progress In Electromagnetics Research Letters*, Vol. 20, 157–163, 2011.
8. Zubir, F., M. K. Abd Rahim, O. B. Ayop, and H. A. Majid,

"Design and analysis of microstrip reflectarray antenna with Minkowski shape radiating element," *Progress In Electromagnetics Research B*, Vol. 24, 317–331, 2010.

9. Capozzoli, A., C. Curcio, G. D'Elia, and A. Liseno, "Fast phase-only synthesis of conformal reflectarrays," *IET Microwaves, Antennas & Propagation*, Vol. 4, No. 12, 1989–2000, 2010.
10. Tienda, C., et al., "Analysis of a dual-reflect array antenna," *IET Microwaves, Antennas & Propagation*, Vol. 5, 1636–1645, 2011.
11. Zainud-Deen, S. H., Hend A. Malhat, and K. H. Awadalla, "Dielectric resonator antenna mounted on a circular cylindrical ground plane," *Progress In Electromagnetics Research B*, Vol. 19, 427–444, 2010.
12. Zainud-Deen, S. H., Hend A. Malhat, and K. H. Awadalla, "Mutual coupling reduction in dielectric resonator antenna arrays embedded in a circular cylindrical ground plane," *Progress in Applied Computational Electromagnetics Society Journal*, Vol. 25, No. 12, 1129–1135, December 2010.
13. Dzulkipli, I., M. H. Jamaluddin, R. Ngah, M. R. Kamarudin, N. Seman, and M. K. Abd Rahim, "Mutual coupling analysis using fdtd for dielectric resonator antenna reflectarray radiation prediction," *Progress In Electromagnetics Research B*, Vol. 41, 121–136, 2012.
14. Jamaluddin, M. H., R. Sauleau, X. Castel, R. Benzerga, L. Le Coq, R. Gillard, and T. Koleck, "Design, fabrication and characterization of a dielectric resonator antenna reflectarray in Ka-band," *Progress In Electromagnetics Research B*, Vol. 25, 261–275, 2010.
15. Nayeri, P., F. Yang, and A. Z. Elsherbeni, "Radiation characteristics of conformal reflectarray antennas," *IEEE International Symposium on Antennas and Propagation*, Spokane, WA, July 2011.
16. Weiland, T., "A discretization method for the solution of Maxwell's equations for six-component fields," *AEU Electronics and Communications*, Vol. 31, No. 3, 116–120, March 1977.
17. Christopoulos, C., *The Transmission Line Modeling Method*, The Institute of Electrical and Electronics Engineers, Inc., 1995.
18. Zhou, X. and G. W. Pan, "Application of physical spline finite element method (PSFEM) to full wave analysis of waveguide," *Progress In Electromagnetics Research*, Vol. 60, 19–41, 2006.